Published in final edited form as:
Eur Heart J. 2008 July ; 29(14): 1721–1728. doi:10.1093/eurheartj/ehn286.

In vivo association between positive coronary artery remodelling and coronary plaque characteristics assessed by intravascular optical coherence tomography

Owen Christopher Raffel[1], **Faisal M. Merchant**[1], **Guillermo J. Tearney**[2], **Stanley Chia**[1], **Denise DeJoseph Gauthier**[1], **Eugene Pomerantsev**[1], **Kyoichi Mizuno**[3], **Brett E. Bouma**[2], and **Ik-Kyung Jang**[1,*]

[1]Cardiology Division, Massachusetts General Hospital and Harvard Medical School, 55 Fruit Street, GRB 800, Boston, MA 02114, USA

[2]Wellman Center for Photomedicine, Massachusetts General Hospital and Harvard Medical School, Boston, MA, USA

[3]Division of Cardiology, Nippon Medical School, Tokyo, Japan

Abstract

Aims—Positive coronary arterial remodelling has been shown to be associated with unstable coronary syndromes and *ex vivo* histological characteristics of plaque vulnerability such as a large lipid core and high macrophage content. The aim of this study is to evaluate the *in vivo* association between coronary artery remodelling and underlying plaque characteristics identified by optical coherence tomography (OCT). OCT is a unique imaging modality capable of characterizing these important morphological features of vulnerable plaque.

Methods and results—OCT and intravascular ultrasound imaging was performed at corresponding sites in patients undergoing catheterization. OCT plaque characteristics for lipid content, fibrous cap thickness, and macrophage density were derived using previously validated criteria. Thin-cap fibroatheroma (TCFA) was defined as lipid-rich plaque (two or more quadrants) with fibrous cap thickness <65 μm. Remodelling index (RI) was calculated as the ratio of the lesion to the reference external elastic membrane area. A total of 54 lesions from 48 patients were imaged. Positive remodelling compared with absent or negative remodelling was more commonly associated with lipid-rich plaque (100 vs. 60 vs. 47.4%, $P = 0.01$), a thin fibrous cap (median 40.2 vs. 51.6 vs. 87 μm, $P = 0.003$) and the presence of TCFA (80 vs. 38.5 vs. 5.6%, $P < 0.001$). Fibrous cap macrophage density was also higher in plaques with positive remodelling showing a positive linear correlation with the RI ($r = 0.60$, $P < 0.001$).

Conclusion—Coronary plaques with positive remodelling exhibit characteristic features of vulnerable plaque. This may explain the link between positive remodelling and unstable clinical presentations.

Keywords

Atherosclerosis; Coronary disease; Coronary remodelling; Optical coherence tomography; Vulnerable plaque

*Corresponding author. Tel: +1 617 726 9226, Fax: +1 617 726 7419, ijang@partners.org.

Conflict of interest: none declared.

Introduction

The coronary arterial wall appears to respond to atheromatous plaque growth by a dynamic process of geometric remodelling that spans the spectrum from outward expansion (positive remodelling) to vessel shrinkage (negative remodelling). It has been hypothesized that positive remodelling occurs in most instances as the initial response to underlying intimal plaque growth, limiting the encroachment of the plaque into the vessel lumen and thereby minimizing luminal stenosis. Paradoxically, this beneficial response is associated with lesions that present with unstable coronary syndromes. Autopsy studies have shown that positive remodelling is associated with underlying lesions with histological characteristics of plaque vulnerability such as a large lipid core and high plaque macrophage content.[1,2]

Intravascular imaging modalities such as intravascular ultrasound (IVUS) and angioscopy do not have the ability to accurately image some of the critical components of high-risk plaque such as fibrous cap thickness and macrophage content. Optical coherence tomography (OCT), however, is a unique high-resolution imaging modality capable of characterizing these important morphological features of atherosclerotic plaque. Using histological controls, the OCT characteristics for components of coronary plaque such as lipid content, fibrous cap thickness, and fibrous cap macrophage density have been validated.[3–5] The aim of this study was to evaluate the *in vivo* association between coronary artery remodelling measured by IVUS and underlying plaque characteristics identified by OCT.

Methods

Study population

Consecutive patients scheduled for cardiac catheterization undergoing percutaneous coronary intervention at Massachusetts General Hospital were screened for the study. Consenting patients with an identifiable culprit lesion in a native coronary artery amenable to percutaneous coronary intervention were subsequently enrolled. Subjects were excluded if they had significant left main coronary artery disease, congestive heart failure, renal insufficiency with baseline serum creatinine > 1.8 mg/dL (> 133 μmol/L), required emergency, or primary angioplasty or had severe stenosis or extremely tortuous or heavily calcified vessels precluding intravascular imaging. IVUS was performed prior to OCT in all cases. Demographic and clinical data were collected prospectively. The institutional review board approved the study, and all patients provided written informed consent before participation.

Lesion identification

The culprit lesion or plaque responsible for the patients clinical syndrome was determined using coronary angiography[6] and corroborated with information from the patient's electrocardiogram, nuclear or echocardiographic stress test, and ventriculogram. Non-culprit (remote) lesions or plaque within the same vessel that were angiographically mild or moderate (30–70% stenosis) were also imaged. Only focal (< 25 mm) non-bifurcating lesions in the native coronary arteries that had not undergone previous percutaneous intervention were imaged.

Intravascular ultrasound and OCT image acquisition

All IVUS and OCT imaging were performed before percutaneous coronary intervention and after the administration of 100–200 μg of intracoronary nitroglycerin. IVUS imaging was performed using a 40 MHz rotational IVUS catheter (Boston Scientific, Natick, MA, USA). The catheter was advanced distal (> 10 mm) to the target lesion up to a distal fiducial landmark documented by contrast angiography and motorized pullback at 0.5 mm/s was then performed

from this point to the aorto-ostial junction. IVUS images were recorded onto 0.5 inch high-resolution super-VHS videotapes for subsequent offline analysis.

The technique of intravascular OCT imaging has been previously described.[4] Prior to introduction into the body, the Z-offset was adjusted to calibrate the imaging catheter to the fiducial marks on the OCT monitor and the intensity of the sheath reflection was used to calibrate detection sensitivity. Using a 0.014 inch guide wire through a 7F guide catheter, a 3.2F OCT catheter was advanced under fluoroscopic guidance to the culprit or remote site. Images were obtained at discrete fixed locations at 4 frames/s (500 angular pixels × 250 radial pixels), during intermittent saline flush (5–10 mL) through the guiding catheter to transiently displace blood. Images were acquired at the area of greatest stenosis or ulceration within the plaque and at its proximal and distal segments and stored digitally for subsequent analysis. The position of the OCT catheter imaging tip at each imaging site was confirmed and documented with contrast fluoroscopy.

By using fluoroscopic reference axial landmarks such as the aorto-ostial junction, proximal and distal side branches, and areas of calcification in combination with the constant imaging pullback speed of the IVUS catheter and the documented precise site of OCT imaging of each plaque, OCT and IVUS image locations of all target sites could be determined and co-registered for analysis.

Intravascular ultrasound image analysis

Two independent operators blinded to the OCT image data analysed the IVUS images. IVUS plaque measurements of external elastic membrane cross-sectional area (EEM CSA) and lumen CSA were performed according to established and validated standards.[7,8] For every patient, the target (culprit and or remote) lesion site and a proximal reference defined as the site with the least amount of plaque < 10 mm proximal to the lesion without any intervening major side branch were selected for measurement. The remodelling index (RI) was defined as the ratio of the lesion EEM CSA to the proximal reference EEM CSA. Positive remodelling was defined as an RI > 1.05, absence of remodelling as an RI of 0.95–1.05, and negative remodelling as an RI < 0.95.[9]

Optical coherence tomography image analysis

All OCT images were analysed by two independent investigators blinded to IVUS image analysis data using previously validated criteria for OCT plaque characterization.[3,5] Images with significant signal attenuation precluding satisfactory evaluation of plaque morphology were excluded from the analysis. The lipid content of a plaque was semi-quantified as the number of involved quadrants on the cross-sectional OCT image. For each plaque, the cross-sectional image with the highest number of lipid quadrants was used for analysis. We have demonstrated previously, using histological controls and the same two investigators, a sensitivity and specificity of 92 and 94%, respectively, to detect lipid-rich plaques using this OCT system. For all images of culprit plaque with an OCT-determined lipid pool, the overlying fibrous cap thickness was measured at its thinnest part. The average of three measurements was taken for each image. For each culprit plaque, the smallest fibrous cap thickness measurement from the three imaging locations was used for subsequent analysis. Histopathological studies show that thin-cap fibroatheroma (TCFA) with evidence of rupture have a large lipid core occupying > 34% of plaque area and a fibrous cap thickness <65 μm.[10] Therefore, if lipid was present in two or more quadrants within a plaque, it was considered as a lipid-rich plaque and TCFAs were defined as lipid-rich plaque with a fibrous cap thickness measuring <65 μm (Figure 1).

Fibrous cap macrophage density was evaluated in all plaques with a lipid pool using a previously validated technique with which we have demonstrated that the OCT-derived macrophage density of plaque fibrous caps correlated strongly (Pearson's correlation coefficient $r = 0.84$, $P < 0.0001$) with macrophage density quantified histomorphometrically by CD68 immunoperoxidase staining in the corresponding histological samples.[5] For each OCT image, the fibrous cap was outlined using automatic bimodal histogram segmentation with the threshold set at the nadir of the bimodal histogram distribution computed from the pixel values within the plaque.[11–13] Lateral boundaries of the cap were marked at the interface between the lipid pool and the adjacent fibrous tissue. Measurement of macrophage content within the fibrous cap was performed on raw OCT data and was expressed as the normalized standard deviation of the OCT signal within the fibrous cap as previously described.[5] For each individual plaque, the value of the highest macrophage density was used for subsequent data analysis. The presence of plaque rupture or thrombus was also evaluated.

Statistical analysis

Continuous variables were reported as means with standard error of means unless otherwise stated. Unpaired *t*-test and the one-way ANOVA test were used for the analysis of continuous variables with normal distribution and Mann–Whitney and Kruskal–Wallis tests were used for the analysis of continuous variables with skewed distribution. The χ^2 test was used for the analysis of categorical variables. Correlation between continuous variables was estimated using Pearson's correlation coefficient. As the distribution of fibrous cap thickness was skewedto the right, natural logarithmic (ln) transformation, which normalized the distribution, was used for the correlation analysis.

All analyses were performed using SPSS version 14 (SPSS Institute Inc.). A $P < 0.05$ was required for statistical significance.

Results

Of 69 lesions or plaque with complete IVUS data that were imaged with OCT, 15 were excluded from the analysis due to OCT signal attenuation (as a result of poor blood clearing or a large burden of intramural thrombus). A total of 54 lesions from 48 patients were analysed for the study. Forty-one (75.9%) were culprit plaques and 13 (24.1%) remote plaques. Twenty (37%) lesions demonstrated positive remodelling, 19 (35.2%) negative remodelling, and 15 (27.8%) absence of remodelling.

Baseline characteristics

The mean age of the cohort was 59 years and 40 (83.3%) were male. The clinical demographics of the patients in relation to lesion remodelling category are presented in Table 1. There were no significant differences in all demographic characteristics between the groups. Although there was a trend toward positively remodelled lesions in patients with acute coronary syndrome (ACS), this finding was not statistically significant.

Remodelling categories and intravascular ultrasound measurements

At the reference site, there were no significant differences between remodelling categories with respect to EEM area, lumen area, and plaque area. At the lesion site, positive remodelling was related to larger EEM, lumen, and plaque area (Table 2).

Remodelling categories and plaque characteristics

The associations between OCT plaque characteristics and remodelling categories are summarized in Table 3. Lipid-rich plaques comprised 100% of positively remodelled lesions

compared with 60% of lesions with absent remodelling and 47.4% of negatively remodelled lesions ($P = 0.01$). A higher plaque lipid content was more often associated with positive remodelling than with absent or negative remodelling ($P = 0.031$ for trend). Plaque that exhibited positive remodelling had a thinner fibrous cap than those plaques with absent or negative remodelling (median 40.2 vs. 51.6 vs. 87.0, respectively, $P = 0.003$).

The macrophage density of the fibrous cap of plaque with positive remodelling was higher than that in plaques with absent and negative remodelling (6.9 vs. 5.7 vs. 3.9, respectively, $P < 0.001$).

Rupture was noted in 11 (24.4%) plaques with a non-significant trend towards a higher incidence of rupture in positively remodelled lesions (Table 3).

Remodelling index and plaque characteristics

When the RI was compared with plaque lipid content, a higher lesion lipid content was associated with a higher mean RI (Figure 2). There was an inverse linear relationship between plaque fibrous cap thickness and the RI ($r = -0.41$, $P = 0.013$; Figure 3A) and a significant positive linear correlation between plaque fibrous cap macrophage density and the RI ($r = 0.60$, $P < 0.001$; Figure 3B). Plaque rupture was non-significantly associated with a higher RI (1.1 vs. 0.97, $P = 0.14$). The presence of thrombus was not related to RI (0.9 vs. 0.9, $P = 0.39$).

Remodelling and thin-cap fibroatheroma

TCFA was not associated with baseline patient demographics or risk factors. There was a significant association between positive remodelling and the presence of underlying plaques that were categorized as TCFA. TCFA comprised 80% of all lesions with positive remodelling, 38.5% of lesions with absent remodelling, and only 5.6% of lesions with negative remodelling (Table 2 and Figure 4, $P < 0.001$). In addition, plaques classified as TCFA were associated with a higher RI compared with plaques that were not TCFA (RI 1.1 vs. RI 0.9, $P < 0.001$).

Discussion

In this study, we examined *in vivo* the association between detailed coronary plaque morphology by OCT and the presence of remodelling identified by IVUS. Our results demonstrate that coronary plaques with positive remodelling exhibit the characteristic features of high-risk plaque thereby both corroborating the results of the previous histopathological *ex vivo* studies and explaining the link between positive remodelling of culprit lesions and an unstable clinical presentation.

Both Smits *et al.*[14], Schoenhagen *et al.*[9], and Nakamura *et al.*[15] demonstrated using IVUS that positive remodelling of the culprit lesion was more often associated with patients who had an unstable vs. a stable coronary syndrome (50 vs. 21.6%, 51.8 vs. 19.6%, and 79.6 vs. 35.2%, respectively). Histopathological studies have shown that the morphology of the underlying plaque is a critical factor in determining its clinical manifestations. Although more than one distinct morphological type of vulnerable plaque has been described, the majority of acute coronary events occur as a result of thrombus formation following disruption of a TCFA; a lesion characterized by a large lipid core overlaid by a thin rupture-prone fibrous cap which is infiltrated with predominantly mononuclear inflammatory cells.[10,16] The relationship between coronary arterial remodelling and underlying plaque morphology was demonstrated in two autopsy studies on subjects of sudden cardiac death.[2,17] Both studies showed that positive remodelling was associated with underlying lesions that demonstrate histological characteristics of plaque vulnerability with larger lipid cores and greater plaque macrophage infiltration than negatively remodelled lesions. However, these were *ex vivo* autopsy studies

on a selected subset of subjects with sudden cardiac death. *In vivo* validation of these findings in a clinically relevant population has been limited, prior to the development of OCT, due to the lack of a sensitive imaging modality to visualize detailed plaque morphology. With this study, we have shown *in vivo* that positive remodelling is associated with plaques with a higher lipid content and greater fibrous cap macrophage density. Indeed a direct linear relationship was noted between the RI and fibrous cap macrophage density. Fibrous cap attenuation is the critical factor predisposing to plaque rupture. There is no data looking at the direct relationship between fibrous cap thickness and remodelling. Burke *et al.*[17] demonstrated that ruptured and unruptured vulnerable plaque (based on a < 65 μm fibrous cap thickness threshold) showed significantly greater positive remodelling than stable plaques (fibrous plaque).We have demonstrated a linear inverse relationship between plaque fibrous cap thickness and the RI (Figure 3A), suggesting that as the degree of outward remodelling increases, fibrous cap attenuation and consequently the risk of fibrous cap rupture with atherothrombosis may increase. In addition, when TCFA was defined as a plaque with fibrous cap thickness <65 μm and two or more lipid quadrants, 80% of positively remodelled lesions were TCFA, whereas only 5.6% of negatively remodelled lesions were TCFA. These results reiterate the association between positive remodelling and plaque vulnerability. Although the reason for this association is not known, it is likely that it is at least in part due to common pathophysiological mechanisms. Macrophage-derived matrix metal-loproteinases (MMPs) are a key factor in the pathogenesis of plaque vulnerability. There is now evidence that MMP activity may play a causal role in positive remodelling.[18,19] Plaque lipid pools are rich in MMPs. The presence of greater macrophage infiltration and higher lipid content in plaques with positive remodelling demonstrated in this study therefore adds *in vivo* support to this pathophysiological concept.

Other intravascular imaging modalities have assessed the relationship between remodelling and plaque morphology *in vivo*. Grey-scale IVUS remains the standard for assessing vessel dimensions and plaque volume and is the modality of choice for evaluating vessel remodelling; however, it is of limited value in evaluating plaque characteristics including plaque lipid content.[20] von Birgelen *et al.*[21] showed that the size of the emptied plaque cavity following cap rupture was larger in lesions with positive remodelling, suggesting that the lipid core in positively remodelled lesions was larger. Spectral analysis of IVUS backscatter radiofrequency data [virtual histology-IVUS (VH-IVUS)] has been used to characterize plaque into morphological tissue components (fibrous, fibrofatty, necrotic core, and dense calcium).[22] However, the results using this technique have been contradictory. Fuji *et al.*[23] showed that lesions with positive remodelling had a larger mean fibrofatty plaque area, whereas the lipid necrotic core area was smaller. Conversely, Rodriguez-Granillo *et al.*[24] demonstrated no difference in fibrofatty area with the mode of remodelling and a larger mean lipid necrotic core area in positively remodelled lesions.[24] Using angioscopy, Smits *et al.*[25] showed that complex plaques with thrombi and yellow colouration (indicating underlying lipid pools) were more frequently observed in positively remodelled lesions. Angioscopy is a qualitative technique and the resolution of current IVUS catheters is in the order of 150 μm and thus both these modalities cannot accurately assess fibrous cap thickness. Recently, VH-IVUS has been used to assess the fibrous cap thickness and identify an IVUS-derived TCFA defined primarily by the lack of fibrous tissue overlying a necrotic core on the radiofrequency derived colour map. However, this assumption is limited not only by the resolution limit of the catheter but also by the analysis window size of ~ 246 μm in the axial direction applied for the colour tissue map reconstruction. In addition, neither angioscopy nor IVUS can measure plaque inflammatory activity. Measurement of plaque temperature and thermal heterogeneity has been shown to correlate with plaque macrophage content. Higher thermal heterogeneity has been demonstrated in positively remodelled lesions in subjects with ACS compared with negatively remodelled lesions.[26] Although all of these modalities have added to our knowledge of the relationship between remodelling and various aspects of plaque morphology *in vivo*, OCT

provides the unique advantage of being able to provide information on the critical aspects of plaque morphology in a single imaging modality.

Limitations

Consecutive subjects who met the eligibility criteria and consented to the study were enrolled. Nevertheless, excluding patients who were unstable, had renal impairment, or calcified vessels may have resulted in a selection bias. However, the enrolment criteria used are common to all studies that require invasive imaging and are necessary for subject safety. In this study, 76% of the plaques were from subjects with an ACS. Therefore, extrapolating to a more general population with a more proportionate representation of coronary syndromes must be done with this in mind. Because of significant attenuation of the emitted infrared light by blood, a blood-free zone is required for OCT imaging. This was achieved through intermittent saline flushes through the coronary guide catheter resulting in short image acquisition times. This enabled imaging only at discrete locations precluding detailed evaluation of entire vessel segments. As a result, only a limited part of the total plaque burden could be sampled. It is therefore possible that we did not image an area of importance such as an exact rupture site within a culprit lesion where fibrous cap attenuation and macrophage infiltration would be greatest. Considering the high prevalence of ACS in our cohort, the frequency of rupture was low. It is likely that due to the discrete imaging method used in this study, the presence of rupture was underestimated. Limited penetration depth (2–3 mm) is another limitation of OCT since, unlike IVUS, it does not enable visualization of the entire plaque or measurements such as plaque volume or the entire lipid pool. However, because the most important morphological determinants of plaque vulnerability are superficial, this region of greatest interest was within the imaging range of the OCT system. Second generation OCT technology currently undergoing development provides significant improvement in image acquisition speed (with frame rates in excess of 100 frames/s) without compromising resolution and image contrast.[25] This development allows continuous imaging of long segments of vessel wall at pullback rates of $\geq$ 20 mm/s, eliminating many of the technical limitations of the present study.

Co-referencing of IVUS and OCT imaging sites was done carefully using landmarks such as side branches and calcified areas along with the motorized pullback speed of IVUS and the documented OCT imaging locations. Nevertheless, it is possible that identical sites were not imaged.

Finally, this was a study in a relatively small cohort and remodelling is a dynamic process so single time point assessments of remodelling using reference segments are not ideal. Further, atherosclerosis is a diffuse process and reference segments that are used often have some plaque burden and may have undergone remodelling. Therefore, the results of this study need to be considered in light of these limitations.

Conclusion

This study provides the first *in vivo* data using OCT that demonstrates the association between remodelling and plaque characteristics. It shows that coronary plaques with positive remodelling exhibit the characteristic features of vulnerable plaque. This corroborates previous *ex vivo* studies and may explain the link between positive remodelling and unstable clinical presentations. Owing to the size and single time-point assessment of this study, prospective longitudinal studies will need to be done on a larger cohort to confirm the robustness of these findings over time and to investigate their clinical significance.

Acknowledgements

We thank our research staff and nurses and technologists at the cardiac catheterization laboratories of Massachusetts General Hospital.

Funding

The study was funded in part by the Center for Integration of Medicine and Innovative Technology (development of the imaging platform), the National Institutes of Health (grant R01-HL70039), Guidant Corporation, and a gift from Dr and Mrs J.S. Chen to the optical diagnostics program of the Wellman Laboratories for Photomedicine. O.C.R. was supported by the White-Parsons fellowship grant awarded by the National Heart Foundation of New Zealand.

References

1. Pasterkamp G, Schoneveld AH, van der Wal AC, Haudenschild CC, Clarijs RJ, Becker AE, Hillen B, Borst C. Relation of arterial geometry to luminal narrowing and histologic markers for plaque vulnerability: the remodeling paradox. J Am Coll Cardiol 1998;32:655–662. [PubMed: 9741507]
2. Varnava AM, Mills PG, Davies MJ. Relationship between coronary artery remodeling and plaque vulnerability. Circulation 2002;105:939–943. [PubMed: 11864922]
3. Yabushita H, Bouma BE, Houser SL, Aretz HT, Jang IK, Schlendorf KH, Kauffman CR, Shishkov M, Kang DH, Halpern EF, Tearney GJ. Characterization of human atherosclerosis by optical coherence tomography. Circulation 2002;106:1640–1645. [PubMed: 12270856]
4. Jang IK, Bouma BE, Kang DH, Park SJ, Park SW, Seung KB, Choi KB, Shishkov M, Schlendorf K, Pomerantsev E, Houser SL, Aretz HT, Tearney GJ. Visualization of coronary atherosclerotic plaques in patients using optical coherence tomography: comparison with intravascular ultrasound. J Am Coll Cardiol 2002;39:604–609. [PubMed: 11849858]
5. Tearney GJ, Yabushita H, Houser SL, Aretz HT, Jang IK, Schlendorf KH, Kauffman CR, Shishkov M, Halpern EF, Bouma BE. Quantification of macrophage content in atherosclerotic plaques by optical coherence tomography. Circulation 2003;107:113–119. [PubMed: 12515752]
6. Ambrose JA, Winters SL, Arora RR, Haft JI, Goldstein J, Rentrop KP, Gorlin R, Fuster V. Coronary angiographic morphology in myocardial infarction: a link between the pathogenesis of unstable angina and myocardial infarction. J Am Coll Cardiol 1985;6:1233–1238. [PubMed: 4067100]
7. Mintz GS, Nissen SE, Anderson WD, Bailey SR, Erbel R, Fitzgerald PJ, Pinto FJ, Rosenfield K, Siegel RJ, Tuzcu EM, Yock PG. American College of Cardiology Clinical Expert Consensus Document on standards for acquisition, measurement and reporting of intravascular ultrasound studies (IVUS). A report of the American College of Cardiology Task Force on Clinical Expert Consensus Documents. J Am Coll Cardiol 2001;37:1478–1492. [PubMed: 11300468]
8. Di Mario C, Gorge G, Peters R, Kearney P, Pinto F, Hausmann D, von Birgelen C, Colombo A, Mudra H, Roelandt J, Erbel R. Study Group on Intracoronary Imaging of the Working Group of Coronary Circulation and of the Subgroup on Intravascular Ultrasound of the Working Group of Echocardiography of the European Society of Cardiology. Clinical application and image interpretation in intracoronary ultrasound. Eur Heart J 1998;19:207–229. [PubMed: 9519314]
9. Schoenhagen P, Ziada KM, Kapadia SR, Crowe TD, Nissen SE, Tuzcu EM. Extent and direction of arterial remodeling in stable versus unstable coronary syndromes: an intravascular ultrasound study. Circulation 2000;101:598–603. [PubMed: 10673250]
10. Virmani R, Kolodgie FD, Burke AP, Farb A, Schwartz SM. Lessons from sudden coronary death: a comprehensive morphological classification scheme for atherosclerotic lesions. (Review) (75 refs). Arterioscler Thromb Vasc Biol 2000;20:1262–1275. [PubMed: 10807742]
11. Gonzalez, RC.; Wintz, PA. Digital Image Processing. Vol. 2nd ed.. Reading, MA: Addison-Wesley; 1987.
12. Jähne, B. Digital Image Processing: Concepts, Algorithms, and Scientific Applications. Vol. 4th ed.. Berlin, New York: Springer; 1997.
13. Pratt, WK. Digital Image Processing: PIKS Inside. Vol. 3rd ed.. New York: Wiley; 2001.
14. Smits PC, Pasterkamp G, Quarles van Ufford MA, Eefting FD, Stella PR, de Jaegere PP, Borst C. Coronary artery disease: arterial remodelling and clinical presentation. Heart 1999;82:461–464. [PubMed: 10490561]

15. Nakamura M, Nishikawa H, Mukai S, Setsuda M, Nakajima K, Tamada H, Suzuki H, Ohnishi T, Kakuta Y, Nakano T, Yeung AC. Impact of coronary artery remodeling on clinical presentation of coronary artery disease: an intravascular ultrasound study. J Am Coll Cardiol 2001;37:63–69. [PubMed: 11153774]

16. Virmani R, Burke AP, Kolodgie FD, Farb A. Vulnerable plaque: the pathology of unstable coronary lesions. J Interv Cardiol 2002;15:439–446. [PubMed: 12476646]

17. Burke AP, Kolodgie FD, Farb A, Weber D, Virmani R. Morphological predictors of arterial remodeling in coronary atherosclerosis. Circulation 2002;105:297–303. [PubMed: 11804983]

18. Pasterkamp G, Schoneveld AH, Hijnen DJ, de Kleijn DP, Teepen H, van der Wal AC, Borst C. Atherosclerotic arterial remodeling and the localization of macrophages and matrix metalloproteases 1, 2 and 9 in the human coronary artery. Atherosclerosis 2000;150:245–253. [PubMed: 10856516]

19. Pasterkamp G, Fitzgerald PF, de Kleijn DP. Atherosclerotic expansive remodeled plaques: a wolf in sheep's clothing. J Vasc Res 2002;39:514–523. [PubMed: 12566977]

20. Peters RJ, Kok WE, Havenith MG, Rijsterborgh H, van der Wal AC, Visser CA. Histopathologic validation of intracoronary ultrasound imaging. J Am Soc Echocardiogr 1994;7:230–241. [PubMed: 8060639]

21. von Birgelen C, Klinkhart W, Mintz GS, Wieneke H, Baumgart D, Haude M, Bartel T, Sack S, Ge J, Erbel R. Size of emptied plaque cavity following spontaneous rupture is related to coronary dimensions, not to the degree of lumen narrowing. A study with intravascular ultrasound in vivo. Heart 2000;84:483–488. [PubMed: 11040004]

22. Nair A, Kuban BD, Tuzcu EM, Schoenhagen P, Nissen SE, Vince DG. Coronary plaque classification with intravascular ultrasound radiofrequency data analysis. Circulation 2002;106:2200–2206. [PubMed: 12390948]

23. Fujii K, Carlier SG, Mintz GS, Wijns W, Colombo A, Bose D, Erbel R, de Ribamar Costa J Jr, Kimura M, Sano K, Costa RA, Lui J, Stone GW, Moses JW, Leon MB. Association of plaque characterization by intravascular ultrasound virtual histology and arterial remodeling. Am J Cardiol 2005;96:1476–1483. [PubMed: 16310425]

24. Rodriguez-Granillo GA, Serruys PW, Garcia-Garcia HM, Aoki J, Valgimigli M, van Mieghem CA, McFadden E, de Jaegere PP, de Feyter P. Coronary artery remodelling is related to plaque composition. Heart 2006;92:388–391. [PubMed: 15964942]

25. Smits PC, Pasterkamp G, de Jaegere PPT, de Feyter PJ, Borst C. Angioscopic complex lesions are predominantly compensatory enlarged: an angioscopy and intracoronary ultrasound study. Cardiovasc Res 1999;41:458–464. [PubMed: 10341845]

26. Toutouzas K, Synetos A, Stefanadi E, Vaina S, Markou V, Vavuranakis M, Tsiamis E, Tousoulis D, Stefanadis C. Correlation between morphologic characteristics and local temperature differences in culprit lesions of patients with symptomatic coronary artery disease. J Am Coll Cardiol 2007;49:2264–2271. [PubMed: 17560291]

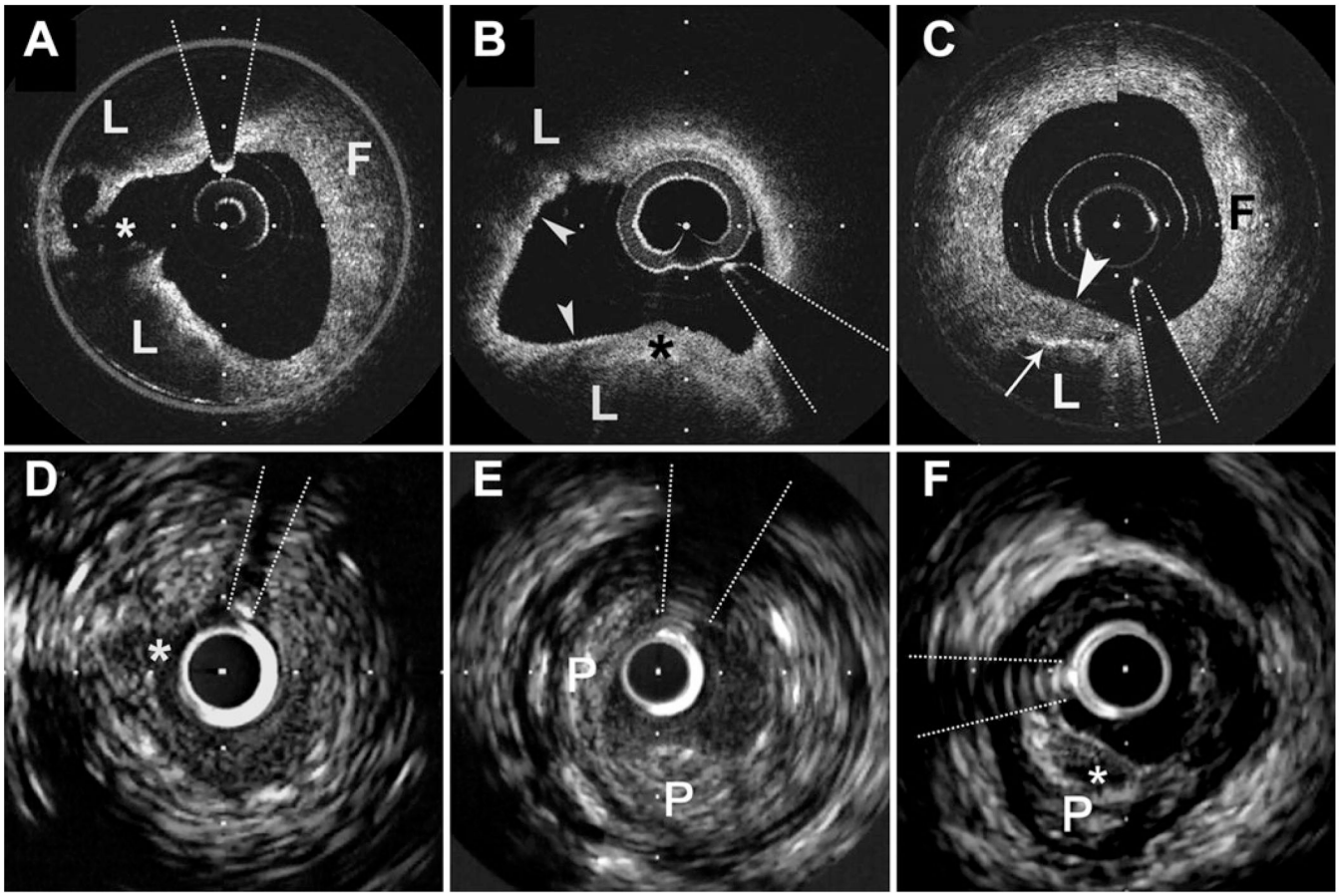

Figure 1.

Optical coherence tomography with corresponding IVUS images of coronary plaque from three subjects. (*A* and *D*) A ruptured plaque from a subject with an acute coronary syndrome. The optical coherence tomography image (*A*) demonstrates a lipid-rich plaque (lipid pools denoted by L, fibrous plaque denoted by F) with evidence of fibrous cap rupture (asterisk). The fibrous cap of this lesion at its thinnest point measured 43 μm. There is a high optical coherence tomography signal with signal heterogeneity within the fibrous cap overlying the lipid pools consistent with high macrophage content. The macrophage content derived from the raw optical coherence tomography signal normal standardized deviation was 6% for the lesion. The corresponding IVUS image shows a luminal defect suggestive of cap disruption; however, clear imaging of the rupture site or the lipid pools with overlying fibrous cap is not evident. Intravascular ultrasound-derived remodelling index was 1.05. (*B* and *E*) A thin-cap fibroatheroma from a subject with an acute coronary syndrome. The optical coherence tomography image demonstrates a lipid-rich plaque (lipid pools denoted by L) with an overlying fibrous cap of variable thickness. In the inferior quadrant of the image, the cap is thick (asterisk) with marked attenuation elsewhere (arrowheads) measuring 39 μm at its thinnest. There is a high optical coherence tomography signal with signal heterogeneity within the fibrous cap consistent with high macrophage content. The macrophage content derived from the raw optical coherence tomography signal normal standardized deviation was 7.9%. The intravascular ultrasound image (*E*) demonstrates the full extent of the plaque (P); however, detailed morphology of the lipid pools, fibrous cap, and inflammatory infiltrate is not possible. The lesion demonstrated positive remodelling with an intravascular ultrasound-derived remodelling index of 1.16. (*C* and *F*) An optical coherence tomography image (*C*) of a

fibroatheroma demonstrating a lipid pool (L) involving only one quadrant underlying a thick fibrous cap (arrowhead) with fibrous tissue (*F*) comprising the other quadrants. High optical coherence tomography signal with signal heterogeneity at the lipid–cap interface (arrow) demonstrates macrophage infiltration. The macrophage density derived from the raw optical coherence tomography signal normalized standardized deviation was 4.6%. The intravascular ultrasound image clearly demonstrates the entire eccentric plaque (P). There is a superficial echo-lucent area (asterisk) suggestive of lipid corresponding to the lipid pool seen on the optical coherence tomography image. Overlying this is an echo-dense line corresponding to the fibrous cap. However, detailed morphology of this area is not evident. Intravascular ultrasound-derived remodelling index was 0.93. The interrupted lines indicate guide-wire artefact. Distance between calibration marks is 500 μm for optical coherence tomography images and 1 mm for IVUS images.

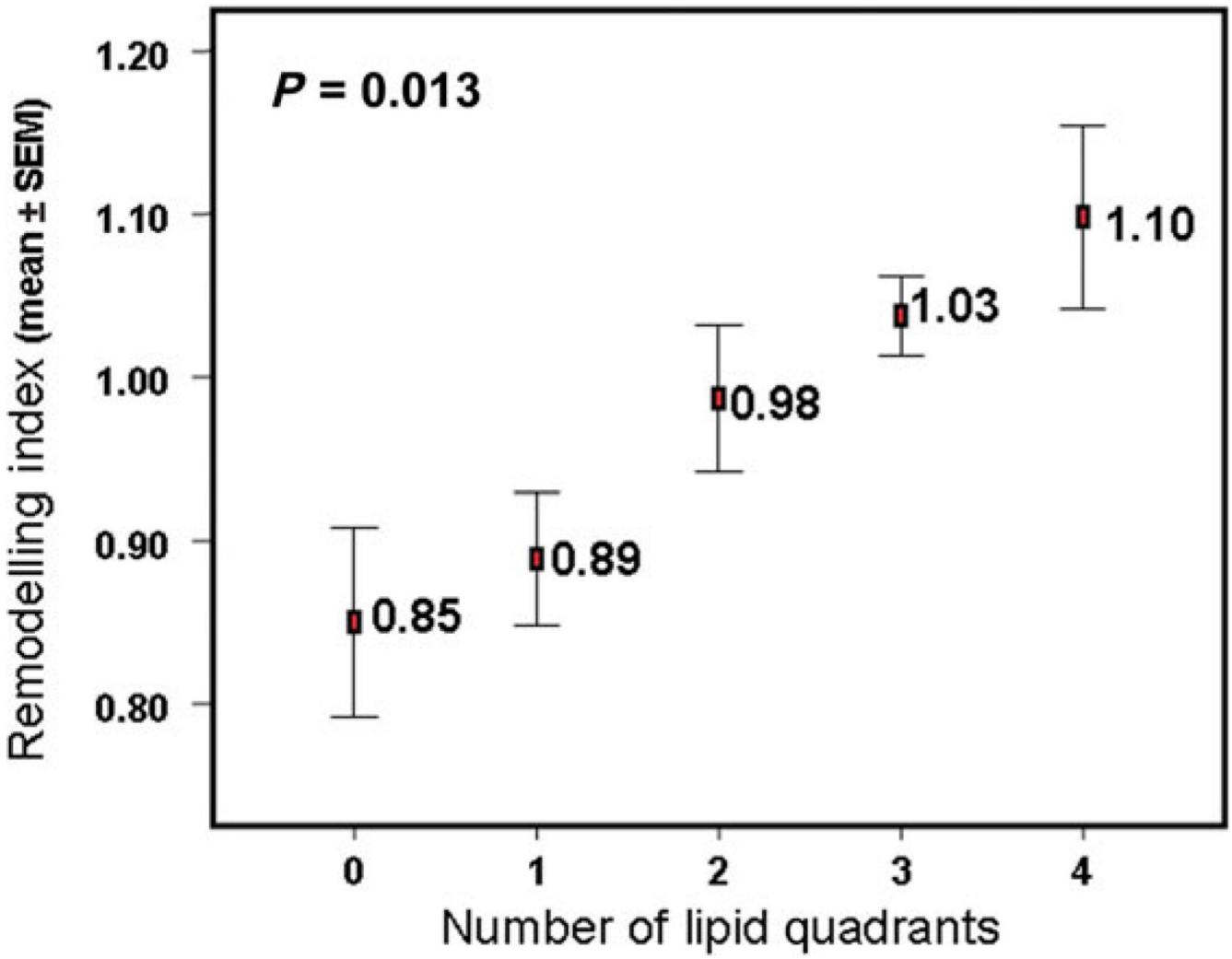

Figure 2.
Association between remodelling index and plaque lipid content assessed as number of involved quadrants in cross-sectional image of the lesion.

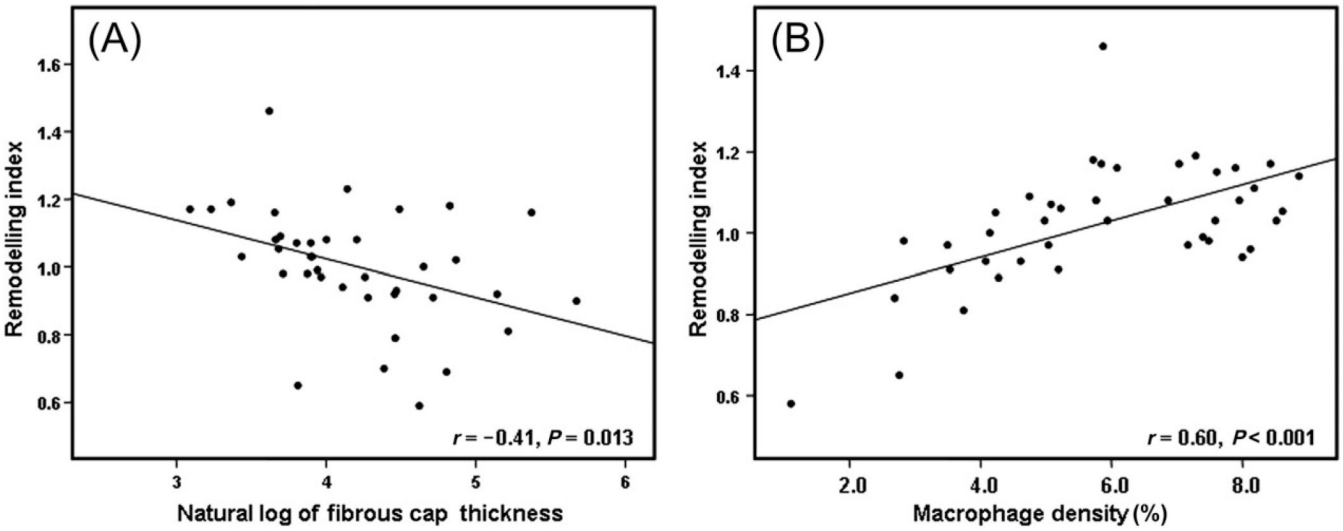

Figure 3.
Scatter plots of (*A*) remodelling index to the logarithm of fibrous cap thickness, (*B*) remodelling index to plaque fibrous cap macrophage density. Pearson's correlation coefficient (*r*) and the *P*-value are depicted in the inset.

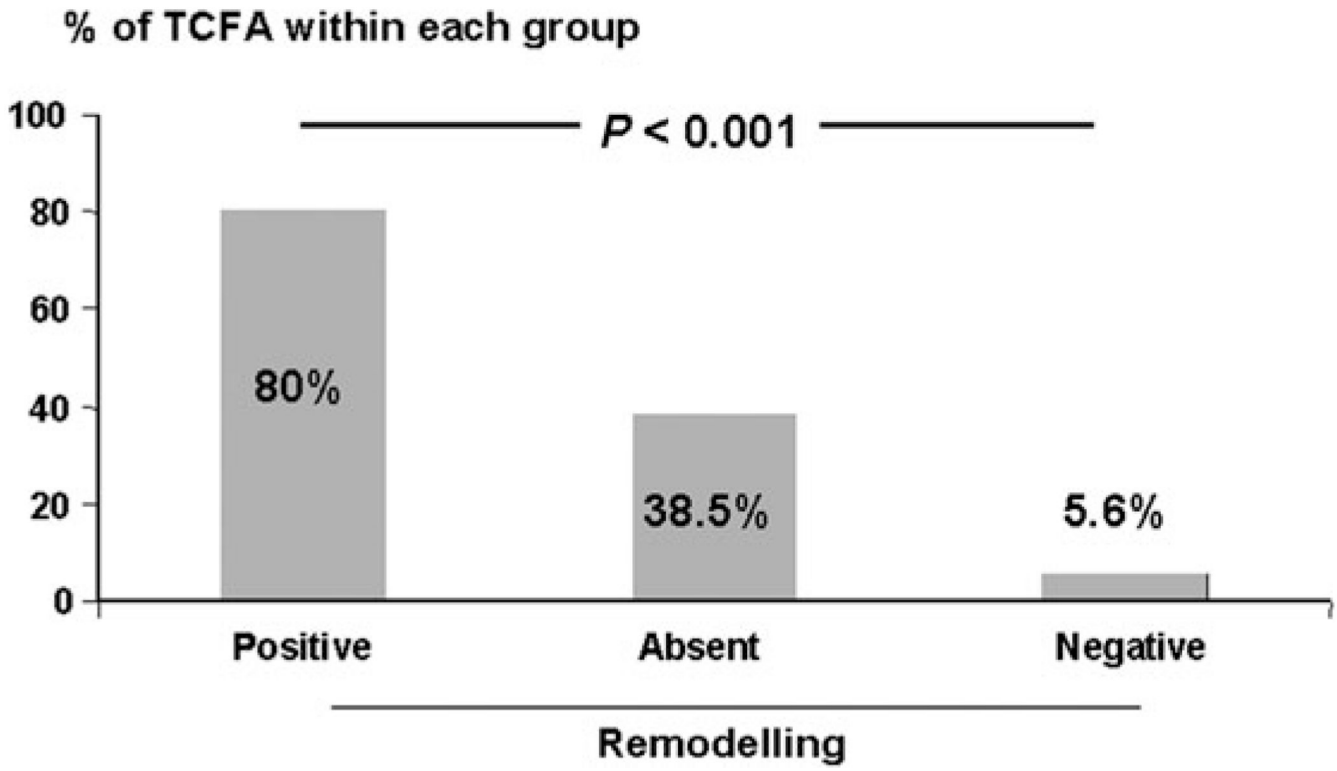

Figure 4.
Frequency of thin-cap fibroatheroma in relation to remodelling category.

Table 1

Baseline clinical demographics and remodelling

Characteristics	RI			*P*-value
	> 1.05 (*n* = 20)	**1.05–0.95 (*n* = 15)**	**< 0.95 (*n* = 19)**	
Age in years, mean (SEM)	57.5 (2.5)	59.2 (2.1)	58.5 (1.3)	0.90
Male sex, *n* (%)	19 (95.0)	12 (80.0)	15 (78.9)	0.30
ACS, *n* (%)	18 (90.0)	9 (60.0)	14 (73.7)	0.12
Smoking history, *n* (%)	16 (80.0)	15 (100)	14 (73.7)	0.11
Dyslipidaemia, *n* (%)	15 (75.0)	8 (53.3)	16 (84.2)	0.13
Diabetes, *n* (%)	4 (20.0)	2 (13.3)	4 (21.1)	0.81
Hypertension, *n* (%)	12(60.0)	9 (60.0)	9 (47.4)	0.67
Culprit lesion, *n* (%)	15 (75.0)	10 (66.7)	16 (84.2)	0.49

ACS, acute coronary syndrome; *n* (%), number (percentage); RI, remodelling index; SEM, standard error of mean.

Table 2

Intravascular ultrasound measurements stratified by remodelling index

IVUS measurement	RI			*P*-value
	> 1.05 (*n* = 20)	**1.05–0.95 (*n* = 15)**	**<0.95 (*n* = 19)**	
Reference				
EEM area (mm^2)	16.5 (0.9)	15.6 (1.2)	15.8 (0.9)	0.80
Lumen area (mm^2)	9.5 (0.6)	9.2 (0.9)	8.9 (0.5)	0.80
Plaque area (mm^2)	13.7 (0.9)	11.6 (1.2)	9.9 (0.6)	0.69
Lesion				
EEM area (mm^2)	18.7 (1.0)	15.6 (1.2)	12.6 (0.7)	0.001
Lumen area (mm^2)	4.5 (0.6)	4.0 (0.4)	2.7 (0.2)	0.011
Plaque area (mm^2)	13.7 (0.9)	11.6 (1.2)	9.9 (0.6)	0.011
Area stenosis (%)	55.9 (4.1)	42.6 (4.5)	68.5 (2.8)	0.010

Values are mean (standard error of mean) unless otherwise stated. IVUS, intravascular ultrasound; EEM, external elastic membrane; RI, remodelling index.

Table 3

Optical coherence tomography plaque characteristics and remodelling index

Plaque characteristics	**RI**			***P*-value**
	> 1.05 (*n* = 20)	**1.05–0.95 (*n* = 15)**	**<0.95 (*n* = 19)**	
Lipid-rich plaque, *n* (%)	20 (100)	9 (60)	9 (47.4)	0.010
Lipid quadrants, *n* (%)				
1	0 (0)	5 (33.3)	6 (31.6)	0.031
2	9 (45.0)	3 (20.0)	5 (26.3)	
3	5 (25.0)	4 (26.7)	2 (10.5)	
4	6 (30.0)	2 (13.3)	2 (10.5)	
Fibrous cap thickness (μm), median (IQR) (*n* = 38)	40.2 (25.5)	51.6 (43.2)	87.0 (84.7)	0.003
TCFA, *n* (%) (*n* = 46)	12 (80.0)	5 (38.5)	1 (5.6%)	<0.001
Macrophage density (NSD%)	6.9	5.7	3.9	<0.001
Rupture, *n* (%)	6 (30.0)	4 (26.7)	1 (5.3)	0.12
Thrombus, *n* (%)	3 (15.0)	5 (33.3)	3 (15.8)	0.34

IQR, inter-quartile range; *n* (%), number (percentage); NSD, normalized standard deviation; RI, remodelling index; TCFA, thin-cap fibroatheroma.